Sensors & Actuators: B. Chemical 305 (2020) 127495

Contents lists available at ScienceDirect

Sensors and Actuators B: Chemical

journal homepage: www.elsevier.com/locate/snb

Electrochemical activation of graphene sheets embedded carbon films for high sensitivity simultaneous determination of hydroquinone, catechol and resorcinol

Liangliang Huang, Yuanyuan Cao, Dongfeng Diao*

Institute of Nanosurface Science and Engineering (INSE), Guangdong Provincial Key Laboratory of Micro/Nano Optomechatronics Engineering, Shenzhen University, Shenzhen, 518060, China

ARTICLE INFO

Keywords:
Carbon film
Graphene sheets
Electrochemical activation
Sensor
Catechol
Resorcinol

ABSTRACT

In this study, the graphene sheets embedded carbon (GSEC) film was electrochemically activated in KOH solution for high sensitivity simultaneous determination of hydroquinone (HQ), catechol (CC) and resorcinol (RC). The electrochemical activation mechanism of GSEC films in alkaline solution was clarified. We found that the embedded graphene sheets were corroded during activation, resulting in the formation of more defective graphene edges and carbonyl functional groups at the surface of carbon film. These corroded graphene edges provided more electrochemical active sites and accelerated the electron transfer. Thus, the activated GSEC film exhibited highly electrocatalytic activity towards the oxidation of HQ, CC and RC. The redox peak separation for HQ and CC decreased from 366 mV to 62 mV and 262 mV to 54 mV, respectively. The oxidation potential of RC also decreased from 714 mV to 590 mV. The electrochemical sensor showed a wide liner response for HQ, CC and RC in the concentration range of 0.5 ~ 200 μM, 0.5 ~ 200 μM and 0.2 ~ 400 μM with detection limit of 0.1 μM, 0.1 μM and 0.05 μM, respectively. These results demonstrate that the KOH-activated GSEC film is a promising electrode material for constructing highly sensitive and selective biosensors.

1. Introduction

Hydroquinone (HQ), catechol (CC) and resorcinol (RC) are three isomers of dihydroxybenzene, which have been widely used in medicines, cosmetics, dyes, tanning, pesticides, photography and chemicals [1]. However, they are considered as environmental pollutants and harmful to human health due to their low degradation rate and high toxicity [2]. The excessive intake of HQ, CC or RC may cause some diseases including fatigue, tachycardia, liver function lesion and even kidney function damage [3,4]. Therefore, developing a reliable analytical method for simultaneous determination of HQ, CC and RC is of great importance. So far, many analytical methods have been exploited to detect them, such as spectrophotometry [5], fluorescence [6], high performance liquid chromatography [7], liquid chromatography-mass spectrometry [8] and electrochemical methods [9]. Among of them, the electrochemical methods have attracted much more attention because of their advantages of low cost, simplicity, time saving, wide linear detection range, high sensitivity and fast response [10]. However, due to the similar structures and properties and usually coexisting of HQ, CC and RC, it's difficult to simultaneous detect them with electrochemical methods. Especially for the HQ and CC, their redox potentials are too close to each other and even overlapping at many electrode materials [10]. To overcome these challenges, many efforts have been devoted to explore new electrode materials for sensitive and simultaneous detection of HQ, CC and RC. Most of these biosensors were prepared by depositing electroactive materials on the glassy carbon, carbon paper or cloth. Their performance mainly depended on the electrochemical activities of electroactive materials, including metal nanoparticles (such as Au [11], Pd [10] and Si [12]), metal oxide (such as PdO [13], NiO [14] and Co_3O_4 [15]), nanocarbon materials (such as graphene [16], N-doped graphene [17], carbon nanotubes [3,18], carbon fiber [19]) and their composites. Some of them realized simultaneous detecting HQ, CC and RC with high sensitivity. However, electrode preparation process of this method is too complicated and not suitable for large-scale manufacturing and application.

Nanocarbon film is a very promising electrode materials for large-scale manufacturing and application in biosensor [20–24]. It possesses wide potential window and low background current, which is beneficial to improve the detection sensitivity. Diao et al [25] prepared a graphene sheets embedded carbon (GSEC) film by using electron cyclotron

* Corresponding author.
E-mail address: dfdiao@szu.edu.cn (D. Diao).

https://doi.org/10.1016/j.snb.2019.127495
Received 8 October 2019; Received in revised form 26 November 2019; Accepted 28 November 2019
Available online 30 November 2019

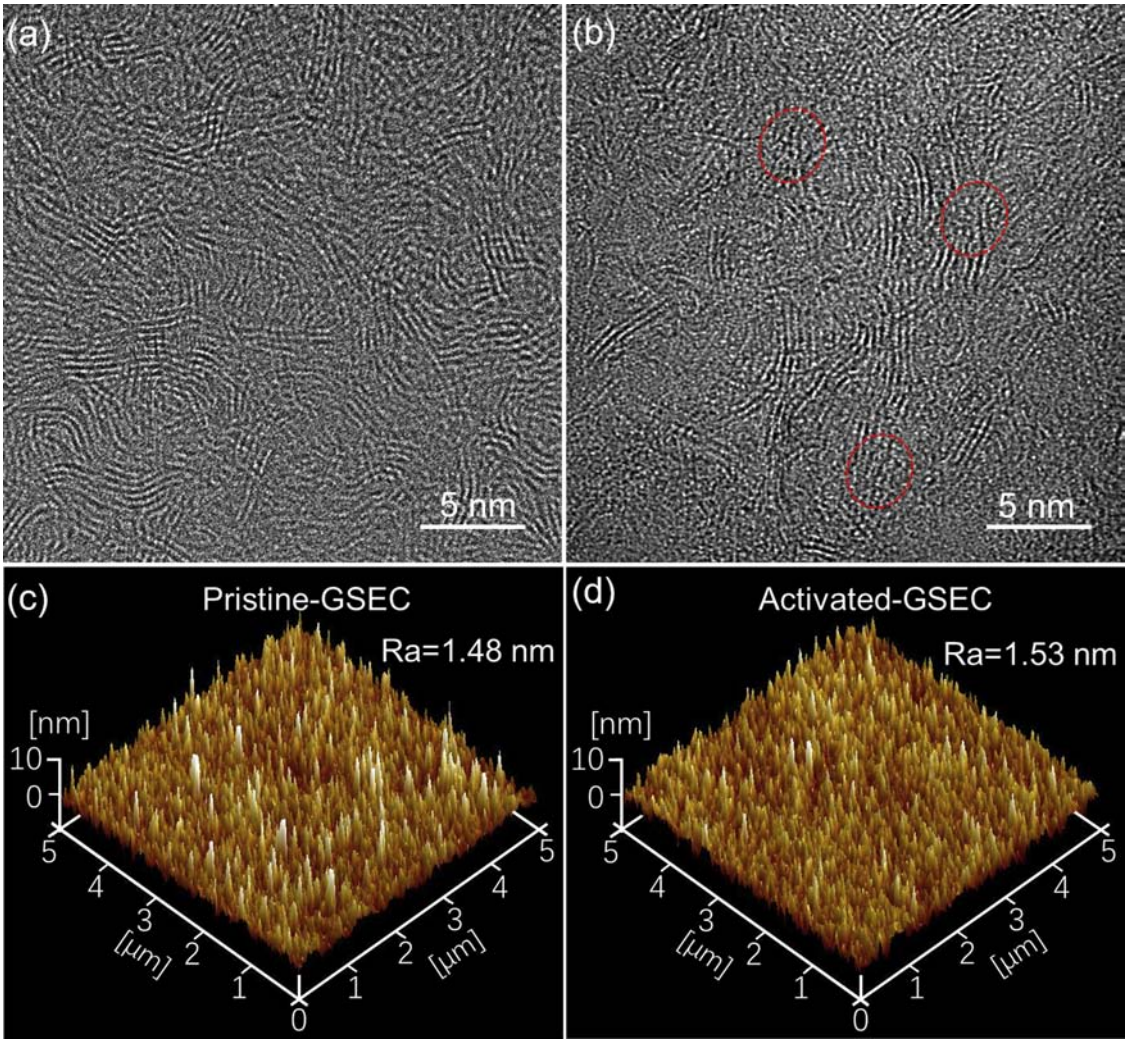

Fig. 1. TEM and AFM images of (a)(c) the pristine GSEC film and (b)(d) activated GSEC film.

resonance (ECR) plasma sputtering under low-energy electron irradiation. By in-situ forming graphene in carbon film, it avoided the agglomeration of graphene and greatly improved the electrochemical activity of carbon films [26–28]. In addition, the vertical graphene sheets induced the high density of graphene edges forming at the film surface, which facilitated the electron transfer between the carbon film and biomolecules. Electrochemical activation is another important method for improving the electrochemical activity of carbon nanomaterials. Most of them were carried out in acid solution by using cyclic voltammetry and potentiostatic method. For example, Wu K et al [29] enhanced the electrochemical activity of N-Methyl-2-pyrrolidone-exfoliated graphene nanosheets for detecting phenols with acetate buffer solution. However, no works have been reported on the electrochemical activation of GSEC in alkaline solution and its application in detecting HQ, CC and RC.

Herein, in this article, the GSEC films were electrochemically activated with cyclic voltammetry in KOH solution, and the electrochemical activities were extremely enhanced. The electrochemical activation mechanism of GSEC film in alkaline solution were clarified. This KOH-activated GSEC films were successfully applied in simultaneous detection of HQ, CC and RC.

2. Experimental

2.1. GSEC film preparation

All GSEC films were deposited on boron-doped silicon wafers (100) with homemade ECR plasma sputtering system as described in our previously published works [26]. Briefly, the Ar was used as working gas and kept a pressure of 4.00×10^{-2} Pa during film preparation. The microwave power and DC voltage applied to the carbon target were kept at 500 W and −500 V, respectively. The electron acceleration voltage was +70 V. The thickness of GSEC films were about 100 nm.

2.2. Electrochemical activation and detection of HQ, CC and RC

Electrochemical workstation (Gamry Reference 600+) was used to perform all electrochemical tests. The counter electrode and reference electrode were a Pt wire and Ag/AgCl, respectively. The electrochemical activation was carried out in 0.1 M KOH solution with cyclic voltammetry (CV) for 12 cycles between 0 ~ 1.2 V vs. Ag/AgCl, which were the optimized activation conditions. The basic electrochemical properties of GSEC films were measured with CV in 1 mM $Fe(CN)_6^{4-/3-}$ in 1 M KCl and 1 mM $Fe^{3+/2+}$ in 0.1 M $HClO_4$ solution. The square wave voltammetry curve (SWVs) of HQ, CC and RC in 0.1 M phosphate buffer solution (PBS) were carried out with a frequency of 5 Hz and a pulse size of 25 mV.

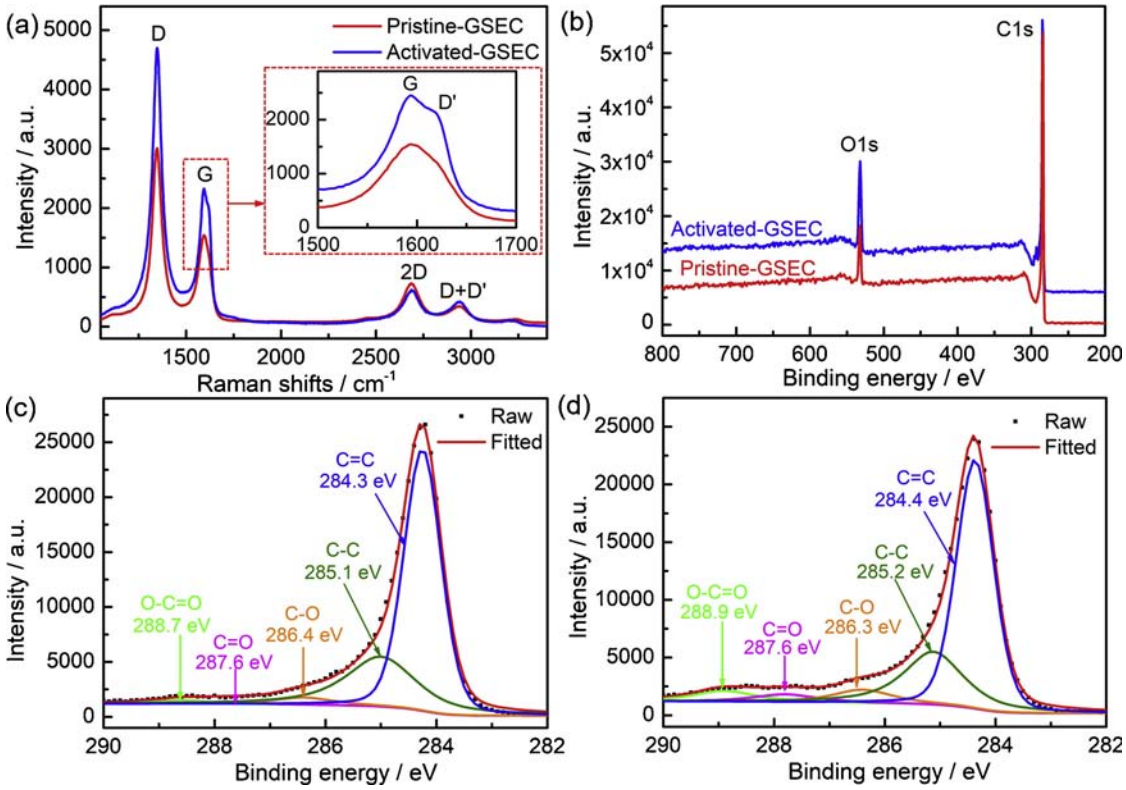

Fig. 2. Raman spectra (a) and XPS spectra (b) of the GSEC carbon films. (c) and (d) are high-resolution decomposition XPS C1 s spectra of the pristine GSEC film and activated GSEC film, respectively.

Table 1
The surface characterization data of GSEC films with Raman and XPS.

	I_D/I_G	$I_{D'}$ (%)	O/C (at.%)	sp^2/sp^3	C1 s (at.%)				
					C = C	C–C	C–O	C = O	O–C = O
Pristine-GSEC	1.97	1.22	10.31	2.20	64.23	29.13	3.78	1.06	1.80
Activated-GSEC	2.34	3.10	16.33	2.31	58.54	25.30	6.52	4.11	5.54

2.3. Film characterization

The surface images of GSEC films were measured by using an atomic force microscopy (AFM) (Dimension Edge) with a BRUKER SCANASYS-AIR tip at room temperature. The scanning rate is 1 Hz with 256 × 256 pixels. A transmission electron microscopy (TEM, Titan3 Themis G2) was used to characterize the nanostructure of carbon films at an electron acceleration voltage of 80 kV. The film surface elemental composition and quantity of chemical bonds were characterized with Raman spectroscopy (HORIBA, Lab RAMHR Evolution) and X-ray photoelectron spectroscopy (XPS, ThermoScientific ESCALAB 250Xi).

3. Results and discussion

3.1. Characterization of activated GSEC

The influences of electrochemical activation on the surface structure and morphology of GSEC films were firstly characterized with TEM and AFM as shown in Fig. 1. The plan view images of TEM showed that many nanosized multilayer graphene sheets were produced in two carbon films. In pristine GSEC film, the multilayer graphene sheets were well organized. But in the activated GSEC film, more defective edges were appeared, such as the red circle area as shown in Fig. 1b. It suggests that some well-organized graphene sheets are damaged/corroded during electrochemical activation in KOH solution. Since the electrochemical corrosion only occurred at the surface of carbon film, the inner structures of carbon film were not changed. The surface electrochemical corrosion caused the formation of more defective graphene edges is beneficial to improve the electrochemical performance. The AFM results showed that the surface roughness of GSEC films increased a little after being electrochemical activated. This slight increase should be resulted from the surface electrochemical corrosion during activation.

For further identifying the defective structures of embedded graphene caused by electrochemical activation, the Raman spectra were measurement, which is the most direct and nondestructive method for characterizing the defects of graphene. As shown in Fig. 2a, the broad 2D bond confirmed the existence of multilayer graphene in two carbon films as characterized by TEM. The D band is related with structural defects and partially the disordered structures of sp^2 carbon, while the G band associated with the degree of graphitization [30,31]. The I_D/I_G is used to assess the level of graphene defects [32]. The intensities of D band and G band both increased obviously after the electrochemical activation, the I_D/I_G also increased from 1.97 to 2.34 as listed in Table 1. It reveals that more defects are formed at the surface of GSEC film by activation. The increased intensity of D + D' band further proves this result. From the insert of Fig. 2a, it can be found that the intensity of D' band is enhanced noticeably by activation. The D' band is associated with the concentration of graphene edge defects [33]. This enhanced D' band indicates that more graphene edge defects are formed

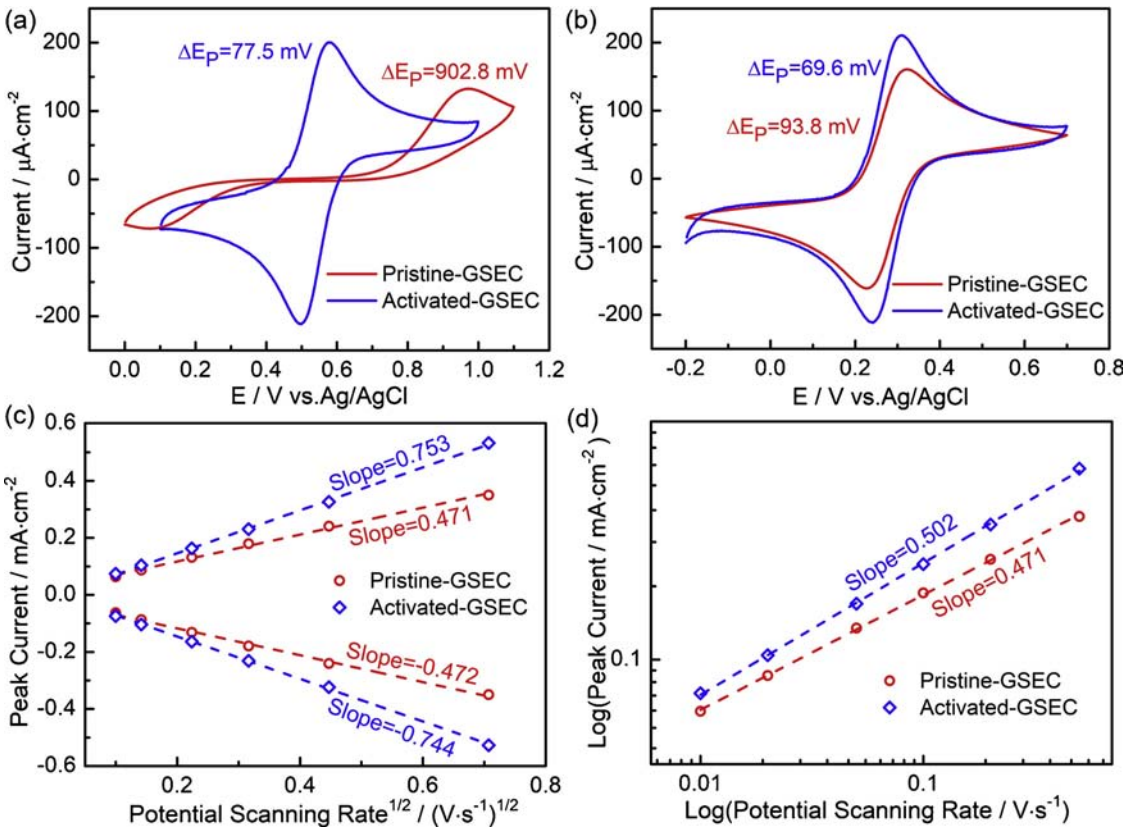

Fig. 3. CVs of GSEC film electrodes in (a) 1 mM $Fe^{3+/2+}$ in 0.1 M $HClO_4$ and (b) 1 mM $Fe(CN)_6^{4-/3-}$ in 1 M KCl with a scan rate of 100 mV/s. (c) Plots of peak current vs scan rate in 1 mM $Fe(CN)_6^{4-/3-}$ and 1 M KCl. (d) Plots of the logarithm of anodic peak current densities vs the logarithm of the scan rate.

at the surface of GSEC films during activation, which is consistent with the TEM results. Therefore, we can conclude that the electrochemical activation results in the formation of more defective graphene edges.

The effects of activation on the surface chemical compositions and bonding structures of GSEC films were probed with XPS as shown in Fig. 2b. It shows that the O/C atomic ratio of GSEC film increases from 10.31 % to 16.33 % after activation. The increase in oxygen content confirms that surface oxides are formed at the surface of GSEC films through electrochemical activation. The high-resolution C 1s peak was fitted into five peaks corresponding to C═C (sp^2), C−C (sp^3), C−O, C═O and O−C = O bonds as shown in Fig.2c and 2d. The carbon bonding compositions were listed in Table 1. It shows that the ratio of sp^2/sp^3 almost remains constant, while the contents of C−O, C═O and O−C═O bonds increase obviously after activation, especially the latter two bonds. The increased C═O and O−C═O bonds indicate the presence of ketone and carboxylic groups in the graphene periphery [34]. These results reflected the fact that most of oxygen functionalities formed during activation were located on the graphene edge sites in GSEC film.

3.2. Basic electrochemical properties

The effects of electrochemical activation on the basic electrochemical properties of GSEC films were characterized with two typical electrochemical probes of $Fe^{3+/2+}$ and $Fe(CN)_6^{4-/3-}$. As shown in Fig. 3a, the redox peak separation ($\triangle E_P$) of $Fe^{3+/2+}$ is 77.5 mV at activated GSEC film, which is much smaller than the value of 902.8 mV obtained at the pristine GSEC film. The redox peak currents at GSEC film also increased obviously after being activated. These results indicate that the KOH-activated GSEC film possesses better electrochemical activity, the electron transfer rate of GSEC film is largely improved by the electrochemical activation. It's well known that the electron transfer rate of $Fe^{3+/2+}$ is sensitive to the presence of surface carbonyl groups on the carbon electrode [35–37]. The XPS results showed that many oxygen functionalities were formed at the graphene edge sites during activation. Therefore, the highly enhanced electron transfer rate of activated GSEC film in $Fe^{3+/2+}$ redox system should be originated from its higher surface oxygen content.

The CVs of 1 mM $Fe(CN)_6^{4-/3-}$ at two carbon films were presented in Fig. 3b. By electrochemical activation, the $\triangle E_P$ of $Fe(CN)_6^{4-/3-}$ decreased form 93.8 mV to 69.6 mV. It indicates that the activated GSEC films have better electrochemical activity than the pristine GSEC films, the electron transfer rate of GSEC film is greatly improved by the electrochemical activation. It is well-established that $Fe(CN)_6^{4-/3-}$ is an inner-sphere redox system, whose kinetics is strongly influenced by the surface chemistry and electronic properties but not "oxide-sensitive" [38]. As proved by McCreery et al. [39–41], the electron transfer rate at the carbon materials electrodes is mainly determined by the content of exposed graphene edges rather than the surface oxygen content. The previous structural analysis showed that the electrochemical activation resulted in much more defective graphene edges formation. More defective graphene edges are beneficial to increase the electronic partial density of states near the Fermi level, and thus, accelerate the electron transfer rate [42,43]. Therefore, the increased defective graphene edges on the surface of GSEC film should be the other reason resulted in the higher electrochemical activity of activated GSEC film.

In addition, the peak current of activated GSEC film is much higher than the pristine GSEC film as shown in Fig. 3b. This may be related with the higher active surface area of activated GSEC film. In order to compare the active surface area of two carbon films, the CVs with different scan rates were measured as shown in Fig. S2. The plots of the peak current as a function of scan rates were depicted in Fig. 3c. The slope of activated GSEC film is higher than that of pristine GSEC film, which indicates the former possesses larger active surface area

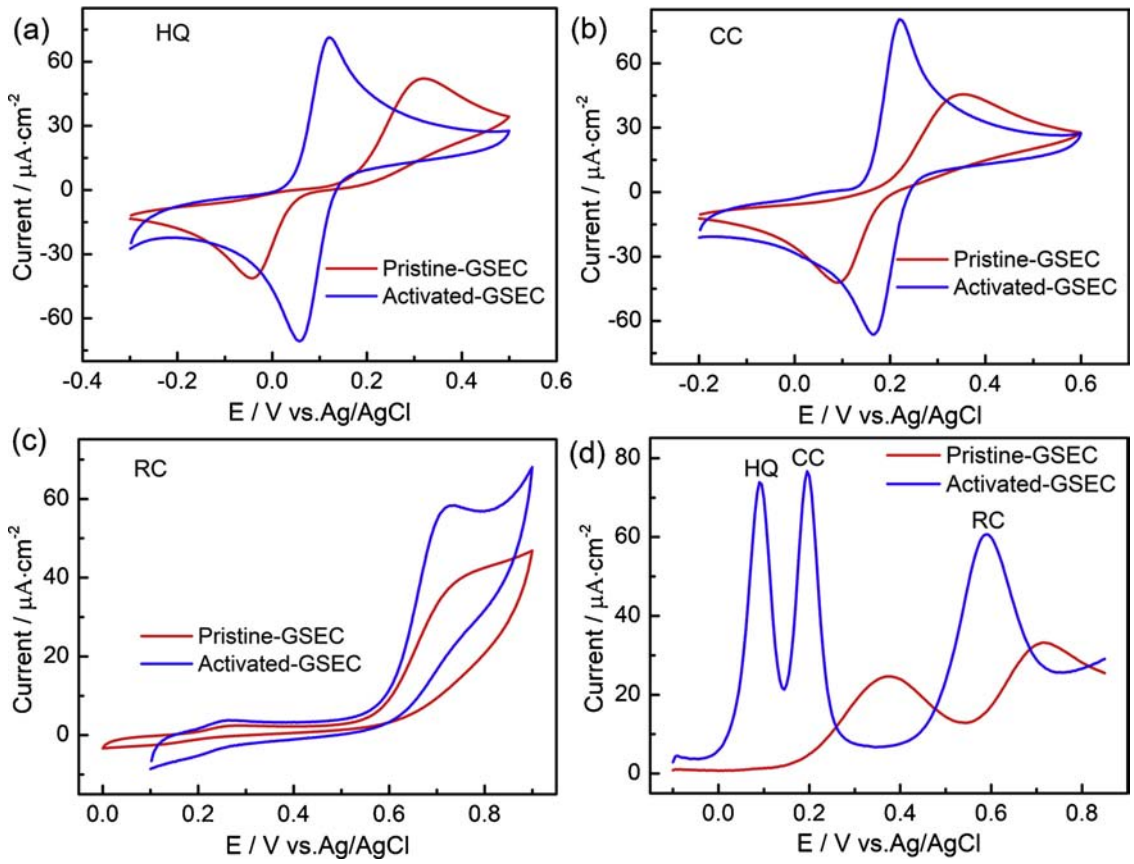

Fig. 4. CVs of GSEC film electrodes in 0.1 M PBS containing (a) 100 μM HQ, (b) 100 μM CC and 100 μM RC, respectively (pH = 7.0, scan rate = 100 mV/s). (d) the SWVs of GSEC film electrodes in 100 μM HQ, 100 μM CC and 200 μM RC in 0.1 M PBS (pH = 7.0).

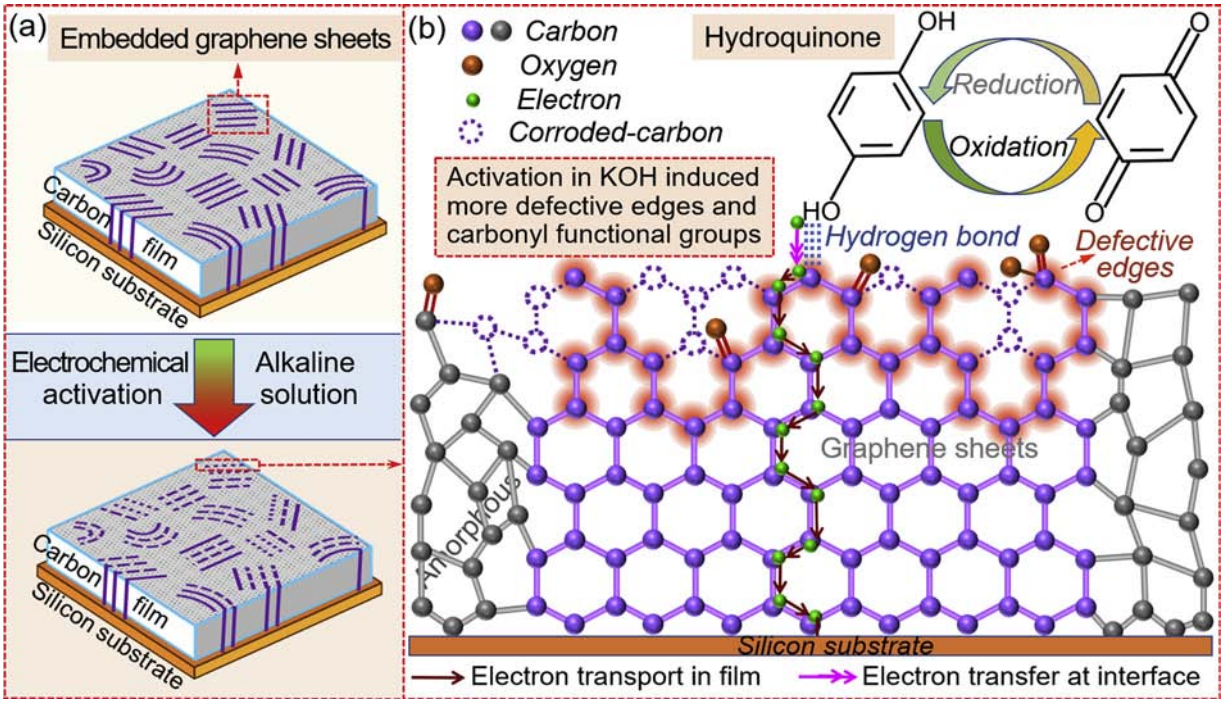

Fig. 5. (a) The electrochemical activation mechanism diagram of GSEC film in KOH solution and (b) the electrocatalytic mechanism of KOH-activated GSEC film for HQ oxidation, the defective edges with higher electronic density of states facilitate the electron transfer between the GSEC film and dihydroxybenzene molecules.

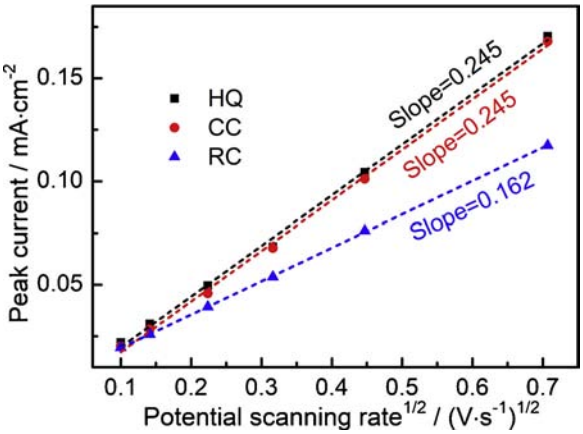

Fig. 6. Plots of oxidation peak currents vs scan rate in 0.1 M PBS (pH = 7.0) contained 100 μM HQ, 100 μM CC and 100 μM RC, respectively.

according to the Randles-Sevcik equation [44]. The activation also increased the surface capacitance (C_{dl}) of GSEC film obviously as showed in Fig S3(a). A linear relation between the logarithm of anodic peak current and logarithm of scan rate was also obtained as shown in Fig. 3d. It means that the redox of $Fe(CN)_6^{4-/3-}$ at the surface of GSEC film is diffusion-control. The slope value of activated GSEC film is closer to the theoretical value of 0.5, further demonstrating that the activated GSEC film has a higher electron transfer rate.

3.3. Electrochemical behaviors of HQ, CC and RC

The individual electrochemical behaviors of HQ, CC and RC at two carbon films were investigated by CV. As shown in Fig. 4a, the electrochemical activation caused a large increase in peak currents of HQ and reduction of $\triangle E_P$, which decreased form 366 mV to 62 mV. Similarly, the activation also increased the peak currents of CC and decreased the $\triangle E_P$ from 262 mV to 54 mV as shown in Fig. 4b. It suggests that the activated GSEC film exhibits well electrocatalytic activity for HQ and CC oxidation. The value of $\triangle E_P$ and oxidation potential for HQ and CC is also lower than some graphene flake-modified electrodes [45,46], which exhibits the high electrochemical activity of activated GSEC films. In addition, the CVs of HQ and CC at activated GSEC films both show good symmetry, which indicates that electron transfer is nearly reversible [47]. For the RC, a clear oxidation peak presented at the KOH-activated GSEC film, but the pristine GSEC film did not. It also proves that the electrochemical reactivity of GSEC films are improved by activation. As only oxidation peak is found in the CV, it is fair to conclude that the oxidation reaction of RC is irreversible. The signal-to-noise (S/N) of two GSEC films in 100 μM HQ, 100 μM CC and 100 μM RC were also measured with SWVs as showed in Fig S3(b). The activated GSEC film exhibits much higher S/N than the pristine GSEC film for HQ and CC although the S/N for RC is slightly reduced.

In order to further compare the effects of activation on the electrochemical activities of GSEC films, the SWVs were characterized in 100 μM HQ, 100 μM CC and 200 μM RC in 0.1 M PBS. As shown in Fig. 4d, only two oxidation peaks present at 375 mV and 714 mV for the oxidation of HQ, CC and RC on the pristine GSEC films electrode. Based on the CVs in Fig. 4a and b, it can be inferred that the oxidation peaks of HQ and CC on the pristine GSEC films electrode are overlapped. So, the pristine GSEC films cannot be applied in determination of HQ, CC and RC. For the activated GSEC film, three well-defined oxidation peaks are shown at 90 mV, 195 mV and 590 mV corresponding to HQ, CC and RC, respectively. Their oxidation peak currents also increased obviously by electrochemical activation. Both the CV and SWV results demonstrate that the electrochemical activities of GSEC films are improved greatly

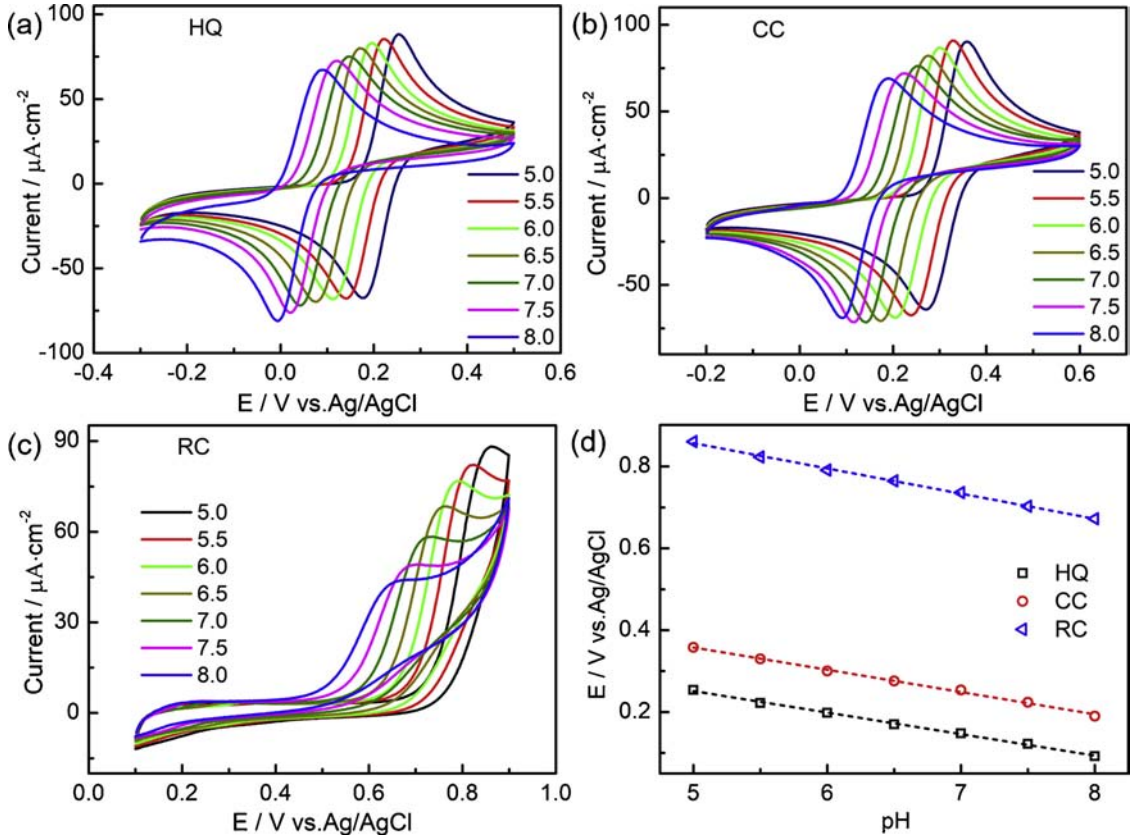

Fig. 7. The CVs of activated GSEC film in three solutions with different pH values: (a) 100 μM HQ + 0.1 M PBS, (b) 100 μM CC + 0.1 M PBS, (c) 100 μM RC + 0.1 M PBS. (d) Plots of effects of anodic peak potential vs pH.

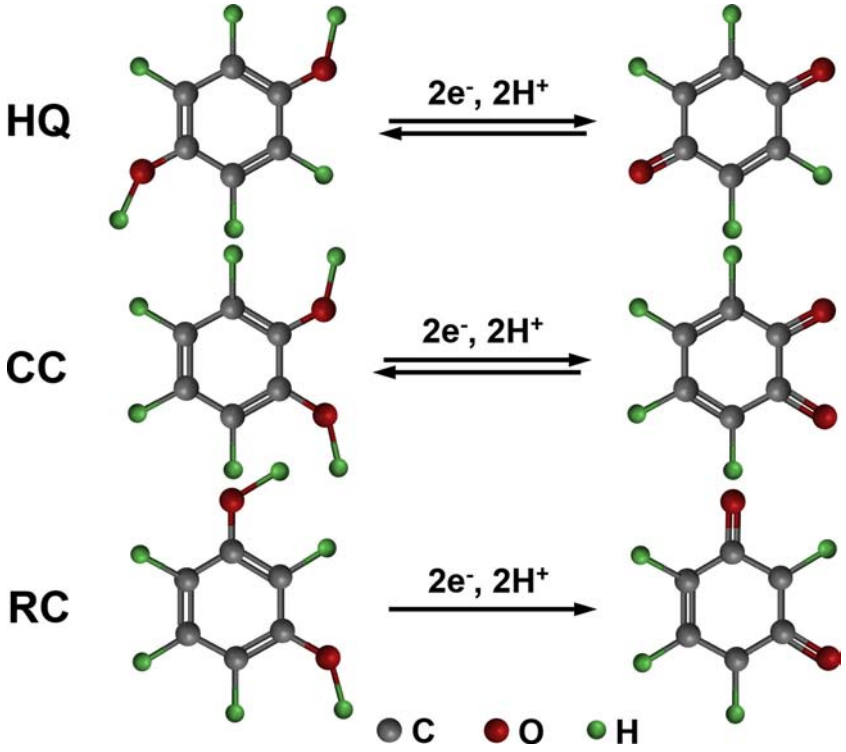

Fig. 8. The electrode reaction mechanisms of HQ, CC and RC.

by activation, and the activated GSEC film can be used to construct electrochemical sensor for simultaneous detecting HQ, CC and RC.

3.4. Mechanisms analysis

The highly improved electrocatalytic activity of GSEC films for detecting HQ, CC and RC is associated with its structural changes during activation in KOH solution. As is known, carbon materials can be oxidized/corroded in alkaline solution when the oxidation potential is high enough, and producing more C═O carbonyl rather than other functional groups [48,49]. During the electrochemical activation of GSEC film in KOH solution, the embedded graphene sheets were oxidized/corroded, resulting in the formation of more defective graphene edges at the carbon film surface as depicted in Fig. 5. These defective graphene edges have higher electronic density of states near the Fermi level [42,50,51], which helping to facilitate the electron transfer between the GSEC film and dihydroxybenzene molecules. Meanwhile, the surface of GSEC film was oxidized during activation and produced more C═O carbonyl functional groups, which further increased the partial density of electronic states and promoted the electron transfer [52]. Therefore, the activated GSEC film showed higher electrochemical activity. In addition, the corroded graphene edges provided more electrochemical active sites. The hydrogen bonds can be more easily formed between hydroxyl in dihydroxybenzene molecules and edge carbon atoms [46,53], thus, promoting the electron transfer between the GSEC film and dihydroxybenzene molecules as shown in Fig. 3b. Consequently, the activated GSEC film exhibited lower $\triangle E_P$ and better electrocatalytic activity for HQ, CC and RC oxidation.

3.5. Effects of scan rate and pH

The effect of scan rate on the electrochemical behavior of HQ, CC and RC was monitored at the activated GSEC film using CV as showed in Fig. S4. With the increasing of potential scan rate, the oxidation peak currents of HQ, CC and RC increase gradually, and the oxidation peak potentials also shift to positive values. It indicates that the electron transfer is quasi-reversible and rapid in the activated GSEC film electrode [17]. As showed in Fig. 6, the oxidation peak currents and square root of scan rates show a linear relation, which demonstrates that the electrode reactions of these three molecules are diffusion-controlled process [54].

The influence of pH values on the response of HQ, CC and RC at activated GSEC film electrode was investigated in the range from 5.0–8.0 as shown in Fig. 7. The oxidation peak current increased slightly with increasing of pH value. This means the KOH-activated GSEC film possesses excellent pH tolerance and responses, which is superior to many other sensor materials [15,17,55]. With increasing of solution pH, the oxidation peak potentials of these three molecules shift negatively. This reveals that protons involve in the oxidation reaction of HQ, CC and RC [54]. The linear relationships of potential of HQ, CC and RC as function of solution pH were expressed as follows:

HQ: E_{pa} (V) = 0.514 – 0.0526 pH (R^2 = 0.998);

CC: E_{pa} (V) = 0.630 – 0.0544 pH (R^2 = 0.997);

RC: E_{pa} (V) = 1.165 – 0.0616 pH (R^2 = 0.998);

The slope values of three equations are close to the theoretical value of −59 mV/pH. According to the Nernst equation [56], it suggests that the electrochemical oxidation of these three molecules at the KOH-activated GSEC film involves the transfer of two electrons and two protons. The electrode reaction mechanisms of HQ, CC and RC were showed in Fig. 8.

3.6. Individual/simultaneous determination of HQ, CC and RC

The electrochemical sensing performance of activated GSEC film towards HQ, CC and RC was investigated by SWV in 0.1 M PBS. For the individual determination of HQ, CC and RC in their mixtures, only the concentration of target species was changed, while the concentrations of the other two species were kept constant as shown in Fig. 9. The peak currents of HQ, CC and RC increased linearly with their concentrations in two concentration ranges. It's also found that the addition of one

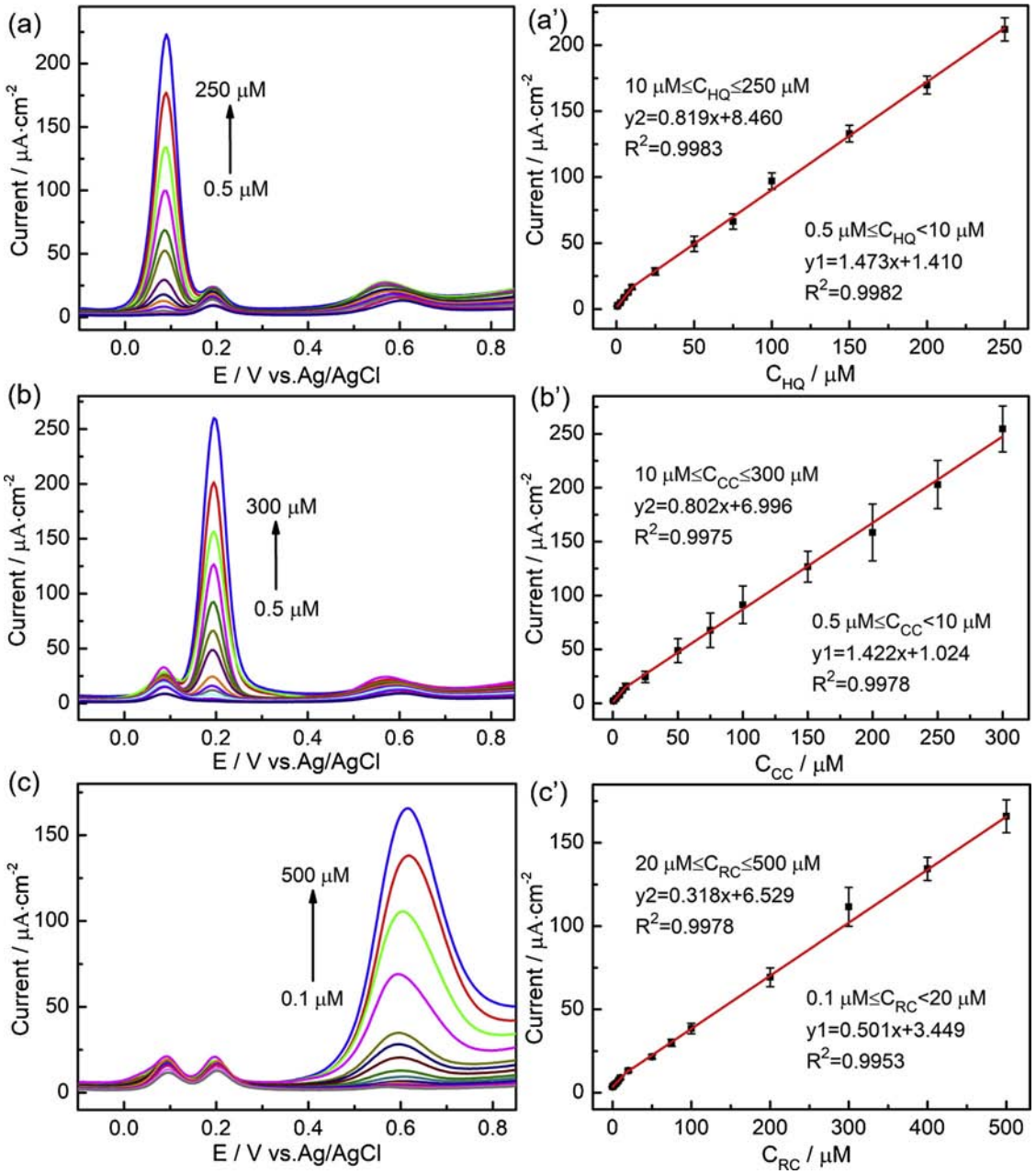

Fig. 9. (a) SWVs of activated GSEC film electrodes in 0.1 M PBS (pH = 7.0) (a) contained 20 μM CC, 40 μM RC and different concentrations of HQ, (b) contained 20 μM HQ, 40 μM RC and different concentrations of CC, (c) contained 20 μM HQ, 20 μM CC and different concentrations of RC. (a')(b')(c') plots of the peak current as a function of HQ, CC and RC concentrations corresponding to (a)(b)(c), respectively.

molecule into the mixture solutions does not generate dramatic influences on the peak potentials and currents of the other two molecules. The linear equations for HQ were $I_{p,\ HQ1} = 1.410 + 1.473C_{HQ}$ (μM) and $I_{p,\ HQ2} = 8.460 + 0.819C_{HQ}$ (μM) in the concentration ranges of 0.5 μM ~ 10 μM and 10 μM ~ 250 μM, respectively. For the CC, the linear equations were $I_{p,\ CC1} = 1.024 + 1.422C_{CC}$ (μM) and $I_{p,\ CC2} = 6.996 + 0.802C_{CC}$ (μM) in the concentration ranges of 0.5 μM ~ 10 μM and 10 μM ~ 300 μM, respectively. For the RC, the linear equations were $I_{p,\ RC1} = 3.449 + 0.501C_{RC}$ (μM) and $I_{p,\ RC2} = 6.529 + 0.318C_{RC}$ (μM) in the concentration ranges of 0.1 μM ~ 20 μM and 20 μM ~ 500 μM, respectively. The detection limits (LOD) of HQ, CC and RC were 0.1 μM, 0.1 μM and 0.05 μM at S/N = 3, respectively. These values are much lower than some [45,53,57] graphene -modified electrodes, it reveals the advantages of activated GSEC film as electrode material in sensing.

The excellent electrochemical activity of activated GSEC film provides a substantial basis for simultaneous determination of HQ, CC and RC. As shown in Fig. 10, three oxidation peaks were well separated, and the oxidation peak currents of HQ, CC and RC still increased linearly with the increasing of their concentrations. Similarly, the oxidation peak current versus concentration of HQ, CC and RC also displayed two different linear response in low concentration and high concentration ranges. This phenomenon could be originated from the formation of a monolayer of adsorbed biomolecules at the electrode surface in low concentration ranges [58,59]. The linear equations and corresponding concentration ranges are as follows:

HQ: $I_{p,\ HQ1} = 2.472 + 1.530C_{HQ}$, 0.5 μM ~ 10 μM; $I_{p,\ HQ2} = 11.123 + 0.658C_{HQ}$, 10 μM ~ 200 μM;

CC: $I_{p,\ CC1} = 1.950 + 1.464C_{CC}$, 0.5 μM ~ 10 μM; $I_{p,\ CC2} = 9.780 + 0.703C_{CC}$, 10 μM ~ 200 μM;

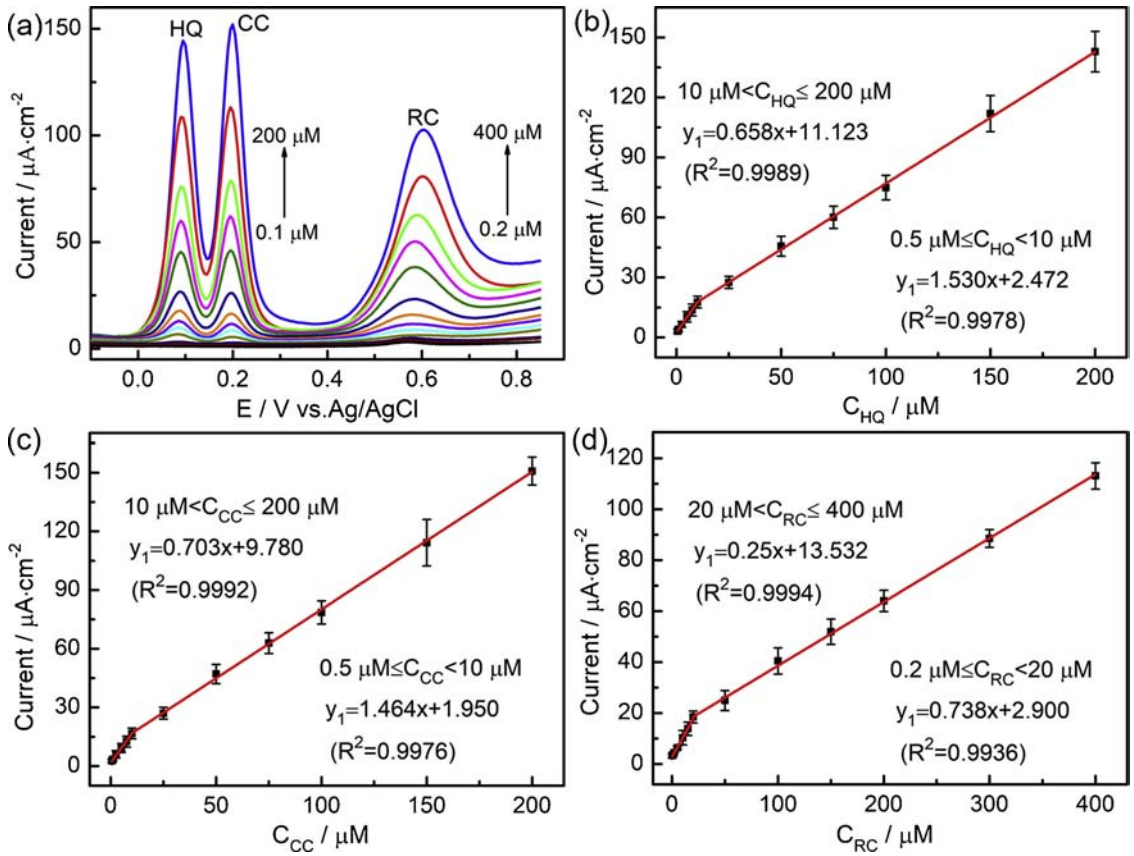

Fig. 10. (a) SWVs of activated GSEC film electrodes in 0.1 M PBS (pH = 7.0) contained different contentrations of HQ, CC and RC. From bottom to up, the concentrations from 0.1 μM to 200 μM for HQ and CC, 0.2 μM–400 μM for RC. (b)(c)(d) Plots of the oxidation peak currents as a function of HQ, CC and RC concentrations, respectively.

Table 2
Comparison of different electrochemical sensors for simultaneous determination of HQ, CC and RC.

Sensing materials	Detection Methods	Linear range /μM			Detection Limit /μM			
		HQ	CC	RC	HQ	CC	RC	
SWCNT/GCE	LSV	2-100	2-100	5-80	0.6	0.6	1.0	[60]
ZnO/graphene	DPV	0-70	0-80	0-700	0.1	0.2	1.0	[61]
Graphene-chitosan/GCE	DPV	1-400	1-550	1-300	0.75	0.75	0.75	[62]
MWCNTs/CDs/MWCNTs/GCE	DPV	1-200	4-200	1-400	0.07	0.06	0.15	[18]
Au-PdNF-NF-PMC/GC	DPV	1.6-100	2.5-100	2.0-100	0.5	0.8	0.7	[10]
ZnO/carbon cloth	CV	2-30	2-45	2-385	0.57	0.81	7.2	[56]
KOH-activated GSEC film	SWV	0.5-200	0.5-200	0.2-400	0.1	0.1	0.05	This work

RC: $I_{p,\ RC1} = 2.900 + 0.738C_{RC}$, 0.2 μM ~ 20 μM; $I_{p,\ RC2} = 13.532 + 0.250C_{RC}$, 20 μM ~ 400 μM.

The LOD of HQ, CC and RC were 0.1 μM, 0.1 μM and 0.05 μM at S/N = 3, respectively. These results are superior/compared to those previously reported results in literature (Table 2). It clearly shows that simultaneous determination of HQ, CC and RC on the activated GSEC films can be achieved with high sensitivity. The stability of the activated GSEC film electrode were characterized with CV in 0.1 M PBS (pH = 7.0) contained 10 μM HQ, 10 μM CC and 20 μM RC as showed in Fig S5. After 25 cycles, the current ratio of HQ is basically not attenuated, the CC and RC are stable above 95 % and 80 %, respectively. It suggests that the stability of activated GSEC film electrodes is well, especially for the HQ and CC. The activated GSEC films with unique structure and electrochemical activity represent a promising electrode material for constructing highly sensitive and selective biosensors.

4. Conclusions

In this study, the electrochemical activation of GSEC films with KOH solution was proposed for highly sensitive simultaneous detecting HQ, CC and RC. We found the embedded graphene sheets were corroded during activation, and more defective graphene edges and carbonyl functional groups were formed at the surface of GSEC film. These corroded graphene edges provided more electrochemical active sites and accelerated the electron transfer between carbon film and redox species. Thus, the activated GSEC film exhibited much better electrochemical activity for the two typical electrochemical probes of $Fe^{3+/2+}$ and $Fe(CN)_6^{4-/3-}$ and higher active surface area than the pristine GSEC film. The activated GSEC film also showed highly electrocatalytic activity towards the oxidation of HQ, CC and RC. The redox peak separation for HQ and CC decreased from 366 mV to 62 mV and 262 mV to 54 mV, respectively. The oxidation potential of RC also decreased from 714 mV to 590 mV. This activated GSEC film could be used to

simultaneous determination of HQ, CC and RC in the concentration range of 0.5 ~ 200 μM, 0.5 ~ 200 μM and 0.2 ~ 400 μM with detection limit of 0.1 μM, 0.1 μM and 0.05 μM, respectively. The KOH-activated GSEC film is a promising electrode material for constructing highly sensitive and selective biosensors.

Declaration of Competing Interest

The authors declare that they have no known competing financial interests or personal relationships that could have appeared to influence the work reported in this paper.

Acknowledgements

This work was supported by the China Postdoctoral Science Foundation (grant numbers 2018M633124); National Nature Science Foundation of China (grant numbers 51975383), and Shenzhen Fundamental Research subject-layout project (grant numbers JCYJ20160427105015701). The authors are also grateful to the Electron Microscopy Center of Shenzhen University for helping in characterization of carbon film nanostructures.

Appendix A. Supplementary data

Supplementary material related to this article can be found, in the online version, at doi:https://doi.org/10.1016/j.snb.2019.127495.

References

[1] W. Si, W. Lei, Y. Zhang, M. Xia, F. Wang, Q. Hao, Electrodeposition of graphene oxide doped poly(3,4-ethylenedioxythiophene) film and its electrochemical sensing of catechol and hydroquinone, Electrochim. Acta 85 (2012) 295–301.
[2] Y. Zhang, G.-M. Zeng, L. Tang, D.-L. Huang, X.-Y. Jiang, Y.-N. Chen, A hydroquinone biosensor using modified core–shell magnetic nanoparticles supported on carbon paste electrode, Biosens. Bioelectron. 22 (2007) 2121–2126.
[3] Y. Wang, Y. Xiong, J. Qu, J. Qu, S. Li, Selective sensing of hydroquinone and catechol based on multiwalled carbon nanotubes/polydopamine/gold nanoparticles composites, Sens. Actuators B Chem. 223 (2016) 501–508.
[4] S. Erogul, S.Z. Bas, M. Ozmen, S. Yildiz, A new electrochemical sensor based on Fe3O4 functionalized graphene oxide-gold nanoparticle composite film for simultaneous determination of catechol and hydroquinone, Electrochim. Acta 186 (2015) 302–313.
[5] Q. Ye, F. Yan, D. Kong, J. Zhang, X. Zhou, J. Xu, L. Chen, Constructing a fluorescent probe for specific detection of catechol based on 4-carboxyphenylboronic acid-functionalized carbon dots, Sens. Actuators B Chem. 250 (2017) 712–720.
[6] H.-P. Wu, T.-L. Cheng, W.-L. Tseng, Phosphate-modified TiO2 nanoparticles for selective detection of dopamine, levodopa, adrenaline, and catechol based on fluorescence quenching, Langmuir 23 (2007) 7880–7885.
[7] Y. Li, C. Yang, J. Ning, Y. Yang, Cloud point extraction for the determination of bisphenol A, bisphenol AF and tetrabromobisphenol A in river water samples by high-performance liquid chromatography, Anal. Methods 6 (2014) 3285–3290.
[8] H. Sambe, K. Hoshina, K. Hosoya, J. Haginaka, Simultaneous determination of bisphenol A and its halogenated derivatives in river water by combination of isotope imprinting and liquid chromatography–mass spectrometry, J. Chromatogr. A 1134 (2006) 16–23.
[9] D. Jiang, J. Pang, Q. You, T. Liu, Z. Chu, W. Jin, Simultaneous biosensing of catechol and hydroquinone via a truncated cube-shaped Au/PBA nanocomposite, Biosens. Bioelectron. 124-125 (2019) 260–267.
[10] Y. Chen, X. Liu, S. Zhang, L. Yang, M. Liu, Y. Zhang, S. Yao, Ultrasensitive and simultaneous detection of hydroquinone, catechol and resorcinol based on the electrochemical co-reduction prepared Au-Pd nanoflower/reduced graphene oxide nanocomposite, Electrochim. Acta 231 (2017) 677–685.
[11] Y. Shen, D. Rao, Q. Sheng, J. Zheng, Simultaneous voltammetric determination of hydroquinone and catechol by using a glassy carbon electrode modified with carboxy-functionalized carbon nanotubes in a chitosan matrix and decorated with gold nanoparticles, Microchimica Acta 184 (2017) 3591–3601.
[12] Fd.M. Morawski, M. Deon, S. Nicolodi, E.W. de Menezes, T.M.H. Costa, S.L.P. Dias, E.V. Benvenutti, L.T. Arenas, Magnetic silica/titania xerogel applied as electrochemical biosensor for catechol and catecholamines, Electrochim. Acta 264 (2018) 319–328.
[13] G. Zheng, Y. Zhang, T. Nie, X. Jiang, Q. Wan, Y. Li, N. Yang, Expanded graphite decorated with PdO@C nanoparticles for individual and simultaneous sensing of multiple phenols, Sens. Actuators B Chem. 291 (2019) 362–368.
[14] L. Zhao, J. Yu, S. Yue, L. Zhang, Z. Wang, P. Guo, Q. Liu, Nickel oxide/carbon nanotube nanocomposites prepared by atomic layer deposition for electrochemical sensing of hydroquinone and catechol, J. Electroanal. Chem. 808 (2018) 245–251.
[15] H. Wang, R. Li, Z. Li, Nanohybrid of Co3O4 and histidine-functionalized graphene quantum dots for electrochemical detection of hydroquinone, Electrochim. Acta 255 (2017) 323–334.
[16] M. Coroş, F. Pogăcean, L. Măgeruşan, M.-C. Roşu, A.S. Porav, C. Socaci, A. Bende, R.-I. Stefan-van Staden, S. Pruneanu, Graphene-porphyrin composite synthesis through graphite exfoliation: the electrochemical sensing of catechol, Sens. Actuators B Chem. 256 (2018) 665–673.
[17] B. Vellaichamy, S.K. Ponniah, P. Prakash, An in-situ synthesis of novel Au@NG-PPy nanocomposite for enhanced electrocatalytic activity toward selective and sensitive sensing of catechol in natural samples, Sens. Actuators B Chem. 253 (2017) 392–399.
[18] C. Wei, Q. Huang, S. Hu, H. Zhang, W. Zhang, Z. Wang, M. Zhu, P. Dai, L. Huang, Simultaneous electrochemical determination of hydroquinone, catechol and resorcinol at Nafion/multi-walled carbon nanotubes/carbon dots/multi-walled carbon nanotubes modified glassy carbon electrode, Electrochim. Acta 149 (2014) 237–244.
[19] Y. Song, T. Yang, X. Zhou, H. Zheng, S.-i. Suye, A microsensor for hydroquinone and catechol based on a poly(3,4-ethylenedioxythiophene) modified carbon fiber electrode, Anal. Methods 8 (2016) 886–892.
[20] O. Niwa, J. Jia, Y. Sato, D. Kato, R. Kurita, K. Maruyama, K. Suzuki, S. Hirono, Electrochemical performance of angstrom level flat sputtered carbon film consisting of sp2 and sp3 mixed bonds, J. Am. Chem. Soc. 128 (2006) 7144–7145.
[21] D. Kato, N. Sekioka, A. Ueda, R. Kurita, S. Hirono, K. Suzuki, O. Niwa, Nanohybrid carbon film for electrochemical detection of SNPs without hybridization or labeling, Angew. Chemie-Int. Ed. 47 (2008) 6681–6684.
[22] D. Kato, N. Sekioka, A. Ueda, R. Kurita, S. Hirono, K. Suzuki, O. Niwa, A nanocarbon film electrode as a platform for exploring DNA methylation, J. Am. Chem. Soc. 130 (2008) 3716–3717.
[23] X. Yang, L. Haubold, G. DeVivo, G.M. Swain, Electroanalytical performance of nitrogen-containing tetrahedral amorphous carbon thin-film electrodes, Anal. Chem. 84 (2012) 6240–6248.
[24] T. Palomäki, N. Wester, L.-S. Johansson, M. Laitinen, H. Jiang, K. Arstila, T. Sajavaara, J.G. Han, J. Koskinen, T. Laurila, Characterization and electrochemical properties of oxygenated amorphous carbon (a-C) films, Electrochim. Acta 220 (2016) 137–145.
[25] W. Chen, X. Zhang, D.F. Diao, Low-energy electron excitation effect on formation of graphene nanocrystallites during carbon film growth process, Appl. Phys. Lett. 111 (2017) 114105.
[26] L. Huang, Y. Cao, D. Diao, Nanosized graphene sheets induced high electrochemical activity in pure carbon film, Electrochim. Acta 262 (2018) 173–181.
[27] L. Huang, Y. Cao, D. Diao, N-doped graphene sheets induced high electrochemical activity in carbon film, Appl. Surf. Sci. 470 (2019) 205–211.
[28] L. Huang, Y. Cao, D. Diao, Surface N-doped graphene sheets induced high electrocatalytic activity for selective ascorbic acid sensing, Sens. Actuators B Chem. 283 (2019) 556–562.
[29] C. Wu, Q. Cheng, K. Wu, Electrochemical functionalization of N-Methyl-2-pyrrolidone-Exfoliated graphene nanosheets as highly sensitive analytical platform for phenols, Anal. Chem. 87 (2015) 3294–3299.
[30] A.C. Ferrari, J.C. Meyer, V. Scardaci, C. Casiraghi, M. Lazzeri, F. Mauri, S. Piscanec, D. Jiang, K.S. Novoselov, S. Roth, A.K. Geim, Raman spectrum of graphene and graphene layers, Phys. Rev. Lett. 97 (2006) 187401.
[31] Z.-H. Sheng, L. Shao, J.-J. Chen, W.-J. Bao, F.-B. Wang, X.-H. Xia, Catalyst-free synthesis of nitrogen-doped graphene via thermal annealing graphite oxide with melamine and its excellent electrocatalysis, ACS Nano 5 (2011) 4350–4358.
[32] K. Chu, J. Wang, Y.-p. Liu, Y.-b. Li, C.-c. Jia, H. Zhang, Creating defects on graphene basal-plane toward interface optimization of graphene/CuCr composites, Carbon 143 (2019) 85–96.
[33] A. Eckmann, A. Felten, I. Verzhbitskiy, R. Davey, C. Casiraghi, Raman study on defective graphene: effect of the excitation energy, type, and amount of defects, Phys. Rev. B 88 (2013) 035426.
[34] T.F. Yeh, C.Y. Teng, S.J. Chen, H. Teng, Nitrogen-doped graphene oxide quantum dots as photocatalysts for overall water-splitting under visible light illumination, Adv. Mater. 26 (2014) 3297–3303.
[35] P.H. Chen, M.A. Fryling, R.L. McCreery, Electron-transfer kinetics at modified carbon electrode surfaces - the role of specific surface sites, Anal. Chem. 67 (1995) 3115–3122.
[36] R.L. McCreery, Advanced carbon electrode materials for molecular electrochemistry, Chem. Rev. 108 (2008) 2646–2687.
[37] S. Ranganathan, R.L. McCreery, Electroanalytical performance of carbon films with near-atomic flatness, Anal. Chem. 73 (2001) 893–900.
[38] P.H. Chen, R.L. McCreery, Control of electron transfer kinetics at glassy carbon electrodes by specific surface modification, Anal. Chem. 68 (1996) 3958–3965.
[39] R.J. Bowling, R.T. Packard, R.L. McCreery, ChemInform abstract: activation of highly ordered pyrolytic graphite for heterogeneous electron transfer: relationship between electrochemical performance and carbon microstructure, ChemInform 20 (1989) no-no.
[40] H. Kaneko, A. Negishi, Y. Suda, T. Kawakubo, Fabrication and evaluation of PFC (PLASTIC formed carbon) electrodes for voltammetric use, Denki Kagaku 61 (1993) 920–921.
[41] C.E. Banks, R.G. Compton, New electrodes for old: from carbon nanotubes to edge plane pyrolytic graphite, Analyst 131 (2006) 15–21.
[42] J.-H. Zhong, J. Zhang, X. Jin, J.-Y. Liu, Q. Li, M.-H. Li, W. Cai, D.-Y. Wu, D. Zhan, B. Ren, Quantitative Correlation between Defect Density and Heterogeneous Electron Transfer Rate of Single Layer Graphene, J. Am. Chem. Soc. 136 (2014) 16609–16617.
[43] R. Sharma, N. Nair, M.S. Strano, Structure − reactivity relationships for graphene nanoribbons, J. Phys. Chem. C 113 (2009) 14771–14777.

[44] A.J. Bard, L.R. Faulkner, Electrochemical Methods: Fundamental and Applications, 2nd ed, John Wiley and Sons New York, 2001.
[45] L. Zheng, L. Xiong, Y. Li, J. Xu, X. Kang, Z. Zou, S. Yang, J. Xia, Facile preparation of polydopamine-reduced graphene oxide nanocomposite and its electrochemical application in simultaneous determination of hydroquinone and catechol, Sens. Actuators B Chem. 177 (2013) 344–349.
[46] Y. Qi, Y. Cao, X. Meng, J. Cao, X. Li, Q. Hao, W. Lei, Q. Li, J. Li, W. Si, Facile synthesis of 3D sulfur/nitrogen co-doped graphene derived from graphene oxide hydrogel and the simultaneous determination of hydroquinone and catechol, Sens. Actuators B Chem. 279 (2019) 170–176.
[47] K. Siuzdak, M. Ficek, M. Sobaszek, J. Ryl, M. Gnyba, P. Niedziałkowski, N. Malinowska, J. Karczewski, R. Bogdanowicz, Boron-enhanced growth of micron-scale carbon-based nanowalls: a route toward high rates of electrochemical biosensing, ACS Appl. Mater. Interfaces 9 (2017) 12982–12992.
[48] Y. Yi, G. Weinberg, M. Prenzel, M. Greiner, S. Heumann, S. Becker, R. Schlögl, Electrochemical corrosion of a glassy carbon electrode, Catal. Today 295 (2017) 32–40.
[49] Y. Yi, J. Tornow, E. Willinger, M.G. Willinger, C. Ranjan, R. Schlögl, Electrochemical degradation of multiwall carbon nanotubes at high anodic potential for oxygen evolution in acidic media, ChemElectroChem 2 (2015) 1929–1937.
[50] A. Ambrosi, A. Bonanni, M. Pumera, Electrochemistry of folded graphene edges, Nanoscale 3 (2011) 2256–2260.
[51] R.J. Bowling, R.T. Packard, R.L. McCreery, Activation of highly ordered pyrolytic graphite for heterogeneous electron transfer: relationship between electrochemical performance and carbon microstructure, J. Am. Chem. Soc. 111 (1989) 1217–1223.
[52] W. Zhang, S. Zhu, R. Luque, S. Han, L. Hu, G. Xu, Recent development of carbon electrode materials and their bioanalytical and environmental applications, Chem. Soc. Rev. 45 (2016) 715–752.
[53] H.-L. Guo, S. Peng, J.-H. Xu, Y.-Q. Zhao, X. Kang, Highly stable pyridinic nitrogen doped graphene modified electrode in simultaneous determination of hydroquinone and catechol, Sens. Actuators B Chem. 193 (2014) 623–629.
[54] Z.-H. Sheng, X.-Q. Zheng, J.-Y. Xu, W.-J. Bao, F.-B. Wang, X.-H. Xia, Electrochemical sensor based on nitrogen doped graphene: simultaneous determination of ascorbic acid, dopamine and uric acid, Biosens. Bioelectron. 34 (2012) 125–131.
[55] H. Jiang, S. Wang, W. Deng, Y. Zhang, Y. Tan, Q. Xie, M. Ma, Graphene-like carbon nanosheets as a new electrode material for electrochemical determination of hydroquinone and catechol, Talanta 164 (2017) 300–306.
[56] S. Meng, Y. Hong, Z. Dai, W. Huang, X. Dong, Simultaneous detection of dihydroxybenzene isomers with ZnO Nanorod/Carbon cloth electrodes, ACS Appl. Mater. Interfaces 9 (2017) 12453–12460.
[57] F. Hu, S. Chen, C. Wang, R. Yuan, D. Yuan, C. Wang, Study on the application of reduced graphene oxide and multiwall carbon nanotubes hybrid materials for simultaneous determination of catechol, hydroquinone, p-cresol and nitrite, Anal. Chim. Acta 724 (2012) 40–46.
[58] A.M. Oliveira-Brett, L.Ad. Silva, C.M.A. Brett, Adsorption of guanine, Guanosine, and Adenine at electrodes studied by differential pulse voltammetry and electrochemical impedance, Langmuir 18 (2002) 2326–2330.
[59] C.M.A. Brett, A.M.O. Brett, Electrochemistry: Principles, Methods, and Applications, Oxford Press, 1993.
[60] Y.-P. Ding, W.-L. Liu, Q.-S. Wu, X.-G. Wang, Direct simultaneous determination of dihydroxybenzene isomers at C-nanotube-modified electrodes by derivative voltammetry, J. Electroanal. Chem. 575 (2005) 275–280.
[61] C. Ge, H. Li, M. Li, C. Li, X. Wu, B. Yang, Synthesis of a ZnO nanorod/CVD graphene composite for simultaneous sensing of dihydroxybenzene isomers, Carbon 95 (2015) 1–9.
[62] H. Yin, Q. Zhang, Y. Zhou, Q. Ma, T. liu, L. Zhu, S. Ai, Electrochemical behavior of catechol, resorcinol and hydroquinone at graphene–chitosan composite film modified glassy carbon electrode and their simultaneous determination in water samples, Electrochim. Acta 56 (2011) 2748–2753.

Liangliang Huang obtained his Ph.D at University of Science and Technology Beijing (China) in 2015, in topics related to materials science and engineering. His present research is focused on the electrochemical sensor and advanced coating materials. He is a former postdoc fellow funded by China Postdoctoral Science Foundation. He is presently an associate researcher at the Nanosurface Science and Engineering (INSE) of Shenzhen University.

Yuanyuan Cao obtained her Ph.D. at Sun Yat-Sen University (China) in 2013, in topics related to the growth mechanism of nanostructure. From 2018 on she works for Institute of Nanosurface Science and Engineering (INSE) of ShenZhen Univetrsity as a lecturer. Her works involves the study of the growth mechanism and the electrochemical properties of nanostructure.

Dongfeng Diao is Head of the Institute of Nanosurface Science and Engineering (INSE) and Electron Microscope Center (EMC) at Shenzhen University. He was awarded a PhD in Mechanical Engineering from Tohoku University in 1992. His research interests include nanosurface science and technology, electrochemical sensors and nanotriboelectronics.